

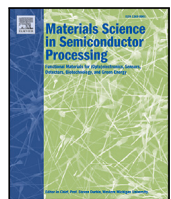


Title	Observation of room-temperature magnetoresistance effect in Co ₂ Fe(Al, Si)/Ge/Co ₂ FeSi vertical spin-valve devices on Si
Author(s)	Watahiki, Shimon; Kusumoto, Shuhei; Yamada, Astuya et al.
Citation	Materials Science in Semiconductor Processing. 2025, 199, p. 109809
Version Type	VoR
URL	https://hdl.handle.net/11094/102338
rights	This article is licensed under a Creative Commons Attribution 4.0 International License.
Note	

The University of Osaka Institutional Knowledge Archive : OUKA

<https://ir.library.osaka-u.ac.jp/>

The University of Osaka



Full length article

Observation of room-temperature magnetoresistance effect in Co₂Fe(Al,Si)/Ge/Co₂FeSi vertical spin-valve devices on Si

Shimon Watahiki ^a, Shuhei Kusumoto ^a, Astuya Yamada ^a, Sora Obinata ^b, Shinya Yamada ^{b,a,c}*^{*}, Shuya Kikuoka ^d, Michihiro Yamada ^d, Kentarou Sawano ^d, Kohei Hamaya ^{b,a,c},

^a Department of Systems Innovation, Graduate School of Engineering Science, The University of Osaka, Toyonaka, Osaka 560-8531, Japan

^b Center for Spintronics Research Network, Graduate School of Engineering Science, The University of Osaka, Toyonaka, Osaka 560-8531, Japan

^c Spintronics Research Network Division, Institute for Open and Transdisciplinary Research Initiatives, The University of Osaka, Suita, Osaka 565-0871, Japan

^d Advanced Research Laboratories, Tokyo City University, Setagaya, Tokyo 158-0082, Japan

ARTICLE INFO

Keywords:

Ge
Sn
Co-based Heusler compounds
Spintronics
Vertical spin-valve devices

ABSTRACT

Using low-temperature growth techniques and an intermediate Ge layer with Sn doping, we experimentally demonstrate an epitaxial Co₂Fe(Al,Si)/Ge/Co₂FeSi heterostructure on a Si platform, where Co₂Fe(Al,Si) and Co₂FeSi are Heusler compounds that exhibit half-metallic properties. The Sn doping only at the initial growth stage of Ge effectively affects the suppression of surface segregation of Sn and the atomic interdiffusion at the Ge/Co₂FeSi heterointerface. By fabricating current-perpendicular-to-the-plane spin-valve devices, we observe a magnetoresistance (MR) effect with an MR ratio of ~0.11 % at room temperature, showing evidence of a nonvolatile memory effect at room temperature, even in a vertical semiconductor spintronic device structure with Co-based Heusler compounds. This study presents crucial findings for high-performance Ge-based vertical spin-valve devices on a Si platform.

1. Introduction

As emerging technologies for low-power semiconductor devices, spin-based transistors [1–15] and spin-based light-emitting diodes (spin LEDs) [16–20] have been extensively explored. Thus far, channel materials, such as GaAs [7,9,10], Si [8,12], Ge [11,13,15], and GaN [14] for the semiconductor spin devices have been considered, but group-IV semiconductors such as Si and Ge are promising for clear spin transport properties above room temperature because of the small spin-orbit interaction derived from the space inversion symmetry in the crystal structure [21,22]. We also demonstrated highly efficient spin injection, transport, and detection in the group-IV semiconductor Ge using lateral and vertically stacked spin-valve device structures [23–27]. Ge not only has higher electron and hole mobilities than Si, but Ge-based technologies are also more promising than Si [28] for future applications such as CMOS [29] and photonic devices [30,31]. In addition, the use of Ge(111) has enabled to grow high-performance ferromagnetic materials, leading to the integration of Ge-based spin devices on a Si platform [11,32].

In general, demonstrating electrical spin injection from ferromagnetic metals (FM) into semiconductors (SC) is difficult because of the

large differences in spin resistance [2,33,34]. One solution for overcoming the spin-resistance mismatch is to use half-metallic materials as spin injectors [34]. In particular, Co-based Heusler compounds have been experimentally shown to enable highly efficient spin injection/detection at room temperature [13,25], facilitating the observation of the two-terminal magnetoresistance (MR) effect at room temperature [26]. Additionally, vertically stacked FM/SC/FM structures are advantageous from the perspective of short-channel implementation and high integration [11,24,35,36]. To date, growth methods for vertically stacked spin-valve (VSV) devices with Ge and the optimization of FM electrodes have been explored [24,27,37–48].

In an early experiment, Fe₃Si with a spin polarization of 0.2 [49] was used as the FM layer, and a high-quality intermediate Ge layer was fabricated using only the temperature gradient molecular beam epitaxy (MBE) method [37]. Subsequently, by combining the SPE and MBE methods, it was possible to obtain sufficient surface flatness with a root-mean-square roughness (R_{rms}) of less than 1 nm [38]. If one of the Co-based Heusler compounds, Co₂FeSi (CFS), with a spin polarization of 0.8 [49] was utilized as the bottom FM layer in the VSV device structure, we experimentally obtained the magnetoresistance (MR)

* Corresponding authors at: Center for Spintronics Research Network, Graduate School of Engineering Science, The University of Osaka, Toyonaka, Osaka 560-8531, Japan.

E-mail addresses: yamada.shinya.es@osaka-u.ac.jp (S. Yamada), hamaya.kohei.es@osaka-u.ac.jp (K. Hamaya).

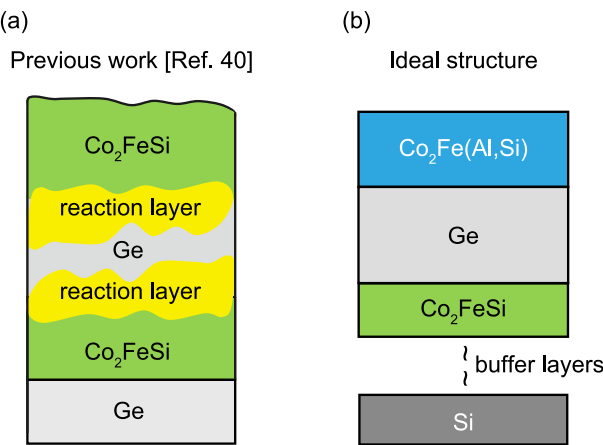


Fig. 1. Schematic of an actual Co_2FeSi (CFS)/Ge/CFS on Ge in Ref. [40] [(a)] and an ideal structure of $\text{Co}_2\text{Fe}(\text{Al},\text{Si})$ (CFAS)/Ge/CFS on Si in this study [(b)].

effect at room temperature [27]. In the field of spintronics, current-perpendicular-to-the-plane giant magnetoresistive [50–52] and tunnel magnetoresistive devices [53,54] with both top- and bottom Co-based Heusler compound electrodes have been already studied. However, it is difficult to simultaneously demonstrate the top Co-based Heusler compound layer on the intermediate Ge in a VSV device structure [Fig. 1(a)] and observe the MR effect at room temperature [40,48].

In this study, we examine a low-temperature-grown Co-based Heusler compound layer, $\text{Co}_2\text{Fe}(\text{Al},\text{Si})$ (CFAS) [23,50,55], as a top FM layer on the intermediate Ge layer. Prior to the CFAS growth, because the intermediate Ge layer obtained by Sn addition was utilized [46,47], the growth conditions of the Sn-doped Ge layer were carefully explored. Consequently, we experimentally demonstrate an ideal structure: an epitaxial CFAS/Ge/CFS heterostructure on Si [Fig. 1(b)]. We also observe the magnetoresistance effect at room temperature by fabricating current-perpendicular-to-the-plane spin-valve devices. This indicates the simultaneous demonstration of epitaxial CFAS/Ge/CFS VSV device structures and the room-temperature MR effect. This study presents important findings for high-performance Ge-based vertical spin-valve devices on a Si platform.

2. Growth of a vertically stacked $\text{Co}_2\text{Fe}(\text{Al},\text{Si})$ /Sn-doped Ge/ Co_2FeSi on Si

In our previous study [40], the growth temperature of the intermediate Ge layer was determined to be 250 °C by utilizing the surfactant effect of Sn, and the only growth method was MBE. As a result, some issues were encountered, including the interfacial reaction between the Co-based Heusler compound and Ge layers, as shown in Fig. 1(a). To improve these features, the growth temperature was further reduced to 110–180 °C by adding 5% Sn during the Ge growth [47]. In this study, we explore a method for Sn doping only at the initial stage of Ge growth and use CFAS as the top FM layer on intermediate Ge, where the lattice mismatch between Ge (~0.564 nm) and CFAS (~0.568 nm) is very small. In the following section, we explain the detailed methods for obtaining the vertically stacked structure shown in Fig. 2(a).

First, as a substrate for the Heusler compounds, a Ge buffer layer was grown in two steps on a Si(111) substrate [32]. Using this substrate for the bottom CFS layer, a 40 nm-thick Fe_3Si layer was grown as a buffer layer on Ge/Si(111) at below 80 °C by low-temperature MBE [27]. The bottom CFS layer was then grown to ~10 nm below 80 °C with low-temperature MBE. The disordered CFS(111) surface was terminated with two atomic layers of Si to form the atomic arrangement of the CFS(111) surface [37]. After confirming the two-dimensional epitaxial surface of the CFS, 5% Sn-doped Ge was deposited using the SPE method (1 nm) to ensure surface flatness [38], followed by

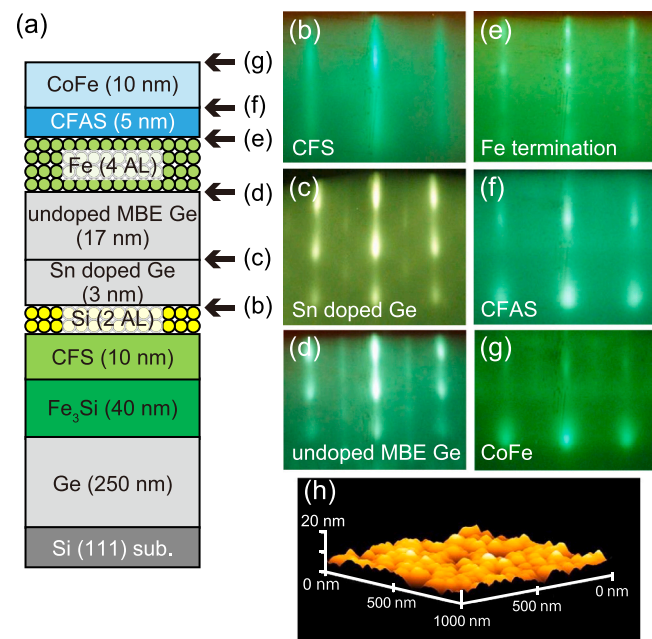


Fig. 2. (a) Schematic of the grown CoFe/CFAS/Sn-doped Ge/CFS/Fe₃Si/Ge on Si(111). [(b)–(g)] RHEED images of the surface for CFS, Sn doped Ge, MBE-Ge, Fe-terminated Ge, CFAS, and CoFe, corresponding to the arrows in Fig. 2(a). (h) AFM image of the surface of the top CoFe layer in the heterostructure.

annealing at 180 °C for approximately 10 min until the amorphous phase disappeared. Subsequently, 5% Sn-doped Ge with a thickness 2 nm was grown at ~180 °C using the MBE method to promote the diffusion of Sn into Ge. Only Ge (without Sn) with a thickness of 17 nm was grown at ~180 °C using the MBE method, and attempts were made to prevent the segregation of Sn. After improving the surface flatness with Fe termination below ~80 °C, the top CFAS layer was grown on top of the Fe-terminated Ge layer below ~80 °C. Finally, we used a CoFe layer as the cap layer to control the coercivity between the top and bottom Co-based Heusler compounds [56].

The crystallinity during growth was examined by observing *in-situ* reflection high-energy electron diffraction (RHEED) images. Fig. 2(b)–2(g) show the RHEED patterns corresponding to the growth steps indicated by the arrows in Fig. 2(a). Fig. 2(b) shows that the surface of the bottom CFS layer was smooth, even after Si termination. In addition, two-dimensional epitaxial growth of a 3-nm-thick Sn-doped Ge layer with 5% Sn doping was achieved [Fig. 2(c)]. After the growth of a 17-nm-thick Ge layer with MBE, the surface maintained a smooth Ge(111) pattern, similar to two-dimensional epitaxial growth [Fig. 2(d)]. The R_{rms} value of the surface of the Ge layer was estimated to be ~1.6 nm from an atomic force microscopy (AFM) image in 1 μm × 1 μm (not shown here). Because of the sufficiently smooth surface, four atomic layers of Fe are epitaxially deposited on top of Ge(111), as shown in Fig. 2(e). The epitaxial growth of the top CFAS layer is shown in Fig. 2(f), followed by the epitaxial CoFe layer with partial spottiness in the RHEED image in Fig. 2(g). Fig. 2(h) shows an AFM image in 1 μm × 1 μm for the surface of the top CoFe layer. The R_{rms} value is estimated to be ~1.7 nm. These results indicate that even with Sn doping, the intermediate Ge layer grown on CFS is of higher quality than that in previous reports [40,47].

3. Structural and magnetic characterizations

High-angle annular dark field (HAADF) scanning transmission electron microscopy (STEM) and energy-dispersive X-ray spectroscopy (EDX) were performed to investigate the structural properties of Sn segregation and interdiffusion at the heterointerface. Fig. 3(a) and (b)

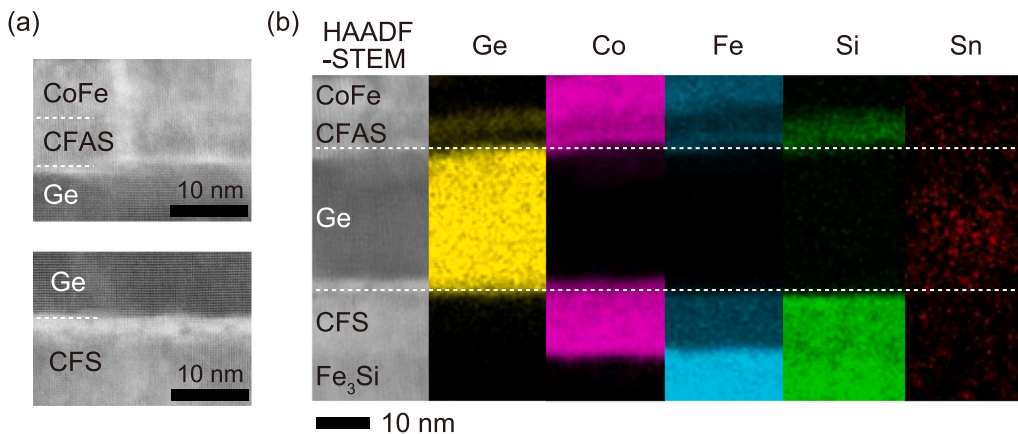


Fig. 3. (a) Cross-sectional high-magnification HAADF-STEM images near the CFAS/Ge and Ge/CFS hererointerfaces. (b) Cross-sectional HAADF-STEM image and EDX elemental maps (Ge, Co, Fe, Si, and Sn) in the same area for a CoFe/CFAS/Sn-doped Ge/CFS/Fe₃Si/Ge on Si(111).

show cross-sectional high-resolution HAADF-STEM images and EDX elemental maps of the vertically stacked CoFe/CFAS/Ge/CFS/Fe₃Si structure on Ge/Si(111), respectively. The left HAADF-STEM image in Fig. 3(b) is the measured area of the EDX elemental maps. From the HAADF-STEM images in Fig. 3(a), we can see that the Ge layer is epitaxially grown on CFS, and the top CoFe/CFAS layer is also epitaxially grown on Ge. These are consistent with the RHEED images shown in Fig. 2. The EDX elemental maps show that CoFe, CFAS, Ge, CFS, and Fe₃Si layers are separately grown. Notably, the doped Sn was observed majorly in the intermediate Ge layer. This indicates that the method of Sn doping only at the initial stage of Ge growth is effective. At the bottom interface between CFS and Ge, atomic interdiffusion between Co and Ge with a several nanometer region is observed. However, at the top interface between CFAS and Ge, the presence of the Fe termination layer at the CFAS/Ge interface can suppress the diffusion of Co into the Ge layer, and the diffusion of Ge into the CFAS layer cannot be fully suppressed at present. Although we need to improve the bottom interface between CFS and Ge and suppress the diffusion of Ge into the CFAS layer, a vertically stacked CFAS/Sn-doped Ge/CFS pseudo-spin-valve structure is experimentally obtained even on Ge/Si(111).

Fig. 4 shows a field-dependent magnetization curve (M - H curve) for an all-epitaxial CoFe/CFAS/Ge/CFS/Fe₃Si structure on Ge/Si(111) measured at room temperature. Clear staircase-like (spin-valve-like) magnetization processes are observed, indicating that the top CoFe/CFAS and bottom CFS/Fe₃Si layers are magnetically decoupled through the intermediate Ge layer. The value of the saturation magnetization is estimated to be ~ 905 emu/cm³, which is slightly smaller than an ideal value (~ 985 emu/cm³) obtained from the estimation of the sum of the values from each FM layer [23,56–58]. This is attributed to the formation of nonmagnetic compounds at the bottom interface of Ge and CFS, in addition to the formation of disordered CFAS(Ge) at the top FM layer. The low-temperature growth in this study enables us to obtain spin-valve-like magnetization reversal processes for an all-epitaxial CoFe/CFAS/Ge/CFS/Fe₃Si structure.

4. MR effect in spin-valve devices

CPP-type spin-valve devices were fabricated to observe spin-dependent transport properties in the all-epitaxial CoFe/CFAS/Ge/CFS/Fe₃Si structure. Fig. 5(a) shows a schematic of the fabricated CPP device and the measurement setup. To fabricate the device, an Au(10 nm)/Ti(3 nm) protective layer was deposited on the top CoFe layer. The bottom FM electrode was patterned using an electron beam lithography system, followed by Ar ion milling to etch the Ge layer on the Si(111) substrate. Next, SiO₂ was deposited via *r*f sputtering to cover the Ge

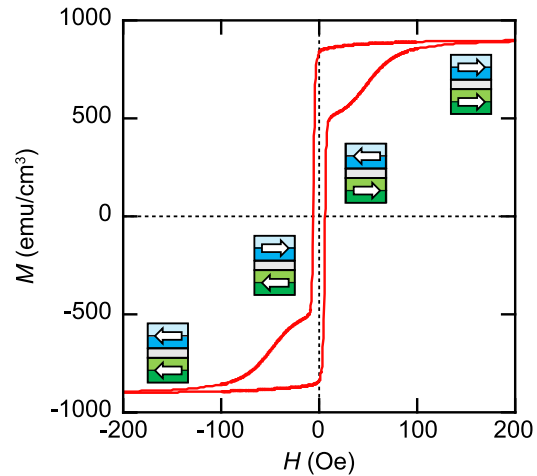


Fig. 4. M - H curve measured at 300 K for a CoFe/CFAS/Sn-doped Ge/CFS/Fe₃Si/Ge/Si(111).

layer. After lift-off, the top FM electrode was patterned using electron-beam lithography and Ar ion milling, where etching was performed down to the Fe₃Si intermediate layer, as shown in Fig. 5(a). To electrically isolate the top and bottom FM electrodes, the entire structure was covered with SiO₂. To electrically connect the top FM layer with the bottom Fe₃Si electrode, we fabricated contact-hole patterns, followed by Ar ion milling to etch the bottom Fe₃Si layer. Finally, the wire-bonded electrode pads were patterned, and ~ 100 nm of Au/Ti was deposited. As shown in Fig. 5(a), the top FM electrode has a hexagonal elongated shape, which introduces shape-induced magnetic anisotropy. The junction size (S) of CoFe/CFAS/Ge/CFS/Fe₃Si in this device is $\sim 5.3 \mu\text{m}^2$.

After connecting the terminals as shown in Fig. 5(a), we measured the two-terminal resistance changes as a function of the external magnetic field (H). Fig. 5(b) and (c) show the representative magnetoresistance as a function of H at 10 and 300 K, respectively. In this study, the two-terminal MR ratio is defined as $(\Delta R_S/R_p) \times 100$, where ΔR_S and R_p are the spin accumulation signal ($\Delta V_S/I$) and the resistance between the FM electrodes through the Ge layer in the parallel magnetization state, respectively. In our devices, $R_p \sim 6.02 \Omega$ at 10 K and $\sim 6.29 \Omega$ at 300 K are close to the values obtained in our previous study [27]. Consequently, at both 10 and 300 K, we clearly observed hysteretic spin signals depending on the parallel and antiparallel magnetization states between the top CoFe/CFAS and bottom CFS/Fe₃Si electrodes, as illustrated in the insets. These features provide

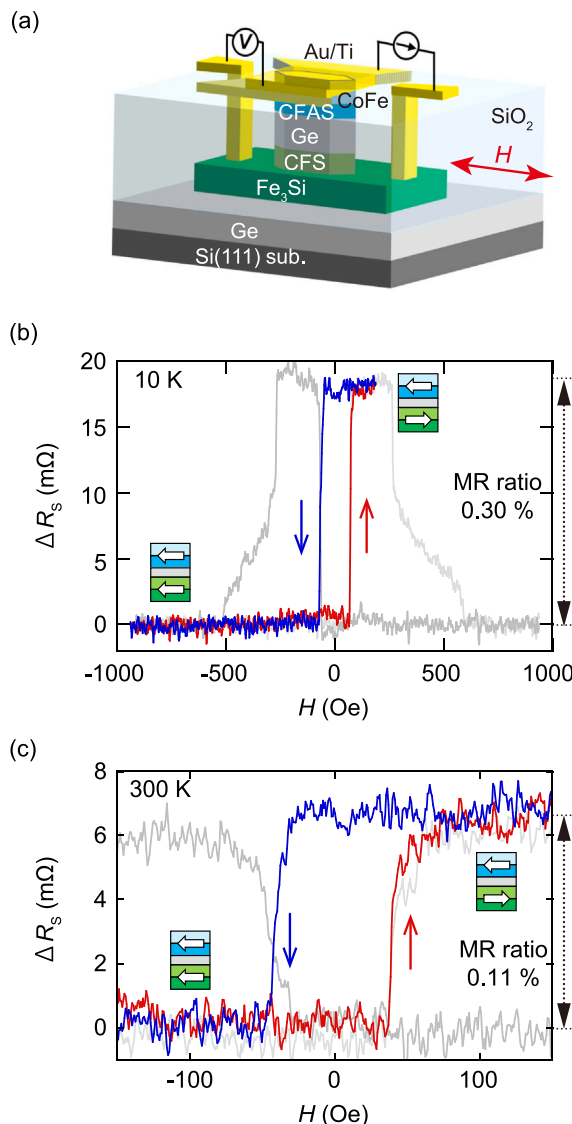


Fig. 5. (a) Schematic of a fabricated VSV device and a measurement terminal configuration. [(b), (c)] Magnetoresistance major hysteresis (gray) and minor (red and blue) loops at 10 and 300 K for a representative VSV device.

evidence of the successful integration of the nonvolatile memory effect into the semiconductor device structures. The values of the spin signal are $\sim 18 \text{ m}\Omega$ at 10 K and $\sim 6.0 \text{ m}\Omega$ at 300 K, corresponding to the MR values of $\sim 0.30\%$ at 10 K and $\sim 0.11\%$ at 300 K, respectively. The room-temperature MR curves were well reproduced in some devices (not shown here). Therefore, we demonstrated epitaxial CFAS/Ge/CFS VSV device structures and observed the room-temperature MR effects.

Finally, we discuss the MR value of $\sim 0.11\%$ at room temperature. Although we utilized Co-based Heusler compound electrodes in the VSV devices, the value was relatively small compared to that in our previous work ($\sim 1.4\%$ [27]). One possible cause is the atomic interdiffusion between Co and Ge in the bottom electrode, as discussed in Section 3. The spin polarization of the interface region at the bottom interface was probably lowered, as expected. In addition, we consider that the formation of the disordered CFAS(Ge) affects the degradation of the spin polarization of the top FM layer. To enhance the MR ratio at room temperature, we should further explore methods for suppressing atomic interdiffusion at the top and bottom Co-based Heusler compound electrodes.

5. Conclusion

Using low-temperature growth techniques and an intermediate Ge layer doped with Sn, we experimentally demonstrated an epitaxial Co₂Fe(Al,Sn)/Ge/Co₂FeSi heterostructure on a Si platform. By fabricating CPP spin-valve devices, we observed the MR effect with an MR ratio of $\sim 0.11\%$ at room temperature, providing evidence of the nonvolatile memory effect at room temperature, even in a vertical semiconductor spintronic device structure with Co-based Heusler compounds. This study presents important findings for high-performance Ge-based vertical spin-valve devices on a Si platform.

CRediT authorship contribution statement

Shimon Watahiki: Writing – original draft, Validation, Investigation, Data curation. **Shuhei Kusumoto:** Investigation. **Astuya Yamada:** Investigation. **Sora Obinata:** Investigation. **Shinya Yamada:** Writing – review & editing, Supervision, Investigation, Data curation. **Shuya Kikuoka:** Resources, Investigation. **Michihiro Yamada:** Resources, Investigation. **Kentarou Sawano:** Resources, Investigation. **Kohei Hamaya:** Writing – review & editing, Supervision, Resources, Project administration, Investigation, Funding acquisition, Data curation, Conceptualization.

Declaration of competing interest

The authors declare that they have no known competing financial interests or personal relationships that could have appeared to influence the work reported in this paper.

Acknowledgments

The authors thank Professors Y. Nakamura and Y. Niimi of The University of Osaka for their experimental support. This work was supported in part by JSPS KAKENHI, Japan (Grant nos. 21H05000, 23KJ1446, 24H00034, 25K01266), JST-CREST, Japan (JPMJCR23A5), JST-Aspire, Japan (Grant no. JPMJAP2413), MEXT X-NICS, Japan (Grant no. JPJ011438), Spintronics Research Network of Japan (Spin-RNJ), Iketani Science and Technology Foundation, Japan, and Masyukainen Basic Research Foundation.

Data availability

Data will be made available on request.

References

- [1] S. Datta, B. Das, Electronic analog of the electro-optic modulator, *Appl. Phys. Lett.* 56 (1990) 665–667.
- [2] A. Fert, H. Jaffr  s, Conditions for efficient spin injection from a ferromagnetic metal into a semiconductor, *Phys. Rev. B* 64 (2001) 184420.
- [3] I.   uti  , J. Fabian, S.D. Sarma, Spintronics: Fundamentals and applications, *Rev. Modern Phys.* 76 (2004) 323.
- [4] A.M. Bratkovsky, Spintronic effects in metallic, semiconductor, metal-oxide and metal-semiconductor heterostructure, *Rep. Prog. Phys.* 71 (2008) 026502.
- [5] H. Dery, P. Dalal, L. Cywi  ski, L.J. Sham, Spin-based logic in semiconductors for reconfigurable large-scale circuits, *Nature* 447 (2007) 573–576.
- [6] M. Tanaka, S. Sugahara, MOS-Based Spin Devices for Reconfigurable Logic, *IEEE Trans. Electron Devices* 54 (2007) 961–976.
- [7] X. Lou, C. Adelmann, S.A. Crooker, E.S. Garlid, J. Zhang, K.S.M. Reddy, S.D. Flexner, C.J. Palmstr  m, P.A. Crowell, Electrical detection of spin transport in lateral ferromagnet-semiconductor devices, *Nat. Phys.* 3 (2007) 197–202.
- [8] I. Appelbaum, B. Huang, D.J. Monsma, Electronic measurement and control of spin transport in silicon, *Nature* 447 (2007) 295–298.
- [9] P. Bruski, Y. Manzke, R. Farshchi, O. Brandt, J. Herfort, M. Ramsteiner, All-electrical spin injection and detection in the Co₂FeSi/GaAs hybrid system in the local and non-local configuration, *Appl. Phys. Lett.* 103 (2013) 052406.
- [10] M. Olttscher, F. Eberle, T. Kuczmik, A. Bayer, D. Schuh, D. Bougeard, M. Ciorga, D. Weiss, Gate-tunable large magnetoresistance in an all semiconductor spin valve device, *Nat. Commun.* 8 (2017) 1807.

- [11] K. Hamaya, Y. Fujita, M. Yamada, M. Kawano, S. Yamada, K. Sawano, Spin transport and relaxation in germanium, *J. Phys. D: Appl. Phys.* 51 (2018) 393001.
- [12] R. Ishihara, Y. Ando, S. Lee, R. Ohshima, M. Goto, S. Miwa, Y. Suzuki, H. Koike, M. Shiraishi, Gate-Tunable Spin XOR Operation in a Silicon-Based Device at Room Temperature, *Phys. Rev. Appl.* 13 (2020) 044010.
- [13] K. Hamaya, M. Yamada, Semiconductor spintronics with Co_2 Heusler compounds, *MRS Bull.* 47 (2022) 584–592.
- [14] S. Yamada, M. Kato, S. Ichikawa, M. Yamada, T. Naito, Y. Fujiwara, K. Hamaya, Half-metallic Heusler Alloy/GaN Heterostructure for Semiconductor Spintronics Devices, *Adv. Electron. Mater.* 9 (2023) 2300045.
- [15] K. Yamamoto, T. Matsuo, M. Yamada, Y. Wagatsuma, K. Sawano, K. Hamaya, Electrical properties of a low-temperature fabricated Ge-based top-gate MOSFET structure with epitaxial ferromagnetic Heusler-alloy Schottky-tunnel source and drain, *Mat. Sci. Semicon. Proc.* 167 (2023) 107763.
- [16] R. Fiederling, M. Keim, G. Reuscher, W. Ossau, G. Schmidt, A. Waag, L.W. Molenkamp, Injection and detection of a spin-polarized current in a light-emitting diode, *Nature* 402 (1999) 787–790.
- [17] Y. Ohno, D.K. Young, B. Beschoten, F. Matsukura, H. Ohno, D.D. Awschalom, Electrical spin injection in a Ferromagnetic Semiconductor Heterostructure, *Nature* 402 (1999) 790.
- [18] A.T. Hanbicki, B.T. Jonker, G. Itskos, G. Kioseoglou, A. Petrou, Efficient electrical spin injection from a magnetic metal/tunnel barrier contact into a semiconductor, *Appl. Phys. Lett.* 80 (2002) 1240–1242.
- [19] S. Iba, H. Saito, S. Yuasa, Y. Yasutake, S. Fukatsu, Fabrication of Ge-based light-emitting diodes with a ferromagnetic metal/insulator tunnel contact, *Japan. J. Appl. Phys.* 54 (2015) 04DM02.
- [20] N. Nishizawa, M. Aoyama, R.C. Roca, K. Nishibayashi, H. Munekata, Arbitrary helicity control of circularly polarized light from lateral-type spin-polarized light-emitting diodes at room temperature, *Appl. Phys. Express* 11 (2018) 053003.
- [21] M.I. Dyakonov, V.I. Perel, Spin Orientation of Electrons Associated with The Interband Absorption of Light in Semiconductors, *Sov. Phys. JETP* 33 (1971) 1053.
- [22] I. Žutić, J. Fabian, S.C. Erwin, Spin Injection and Detection in Silicon, *Phys. Rev. Lett.* 97 (2006) 026602.
- [23] Y. Fujita, M. Yamada, M. Tsukahara, T. Oka, S. Yamada, T. Kanashima, K. Sawano, K. Hamaya, Spin Transport and Relaxation up to 250 K in Heavily Doped *n*-type Ge Detected Using $\text{Co}_2\text{FeAl}_{0.5}\text{Si}_{0.5}$ Electrodes, *Phys. Rev. Appl.* 8 (2017) 014007.
- [24] M. Kawano, M. Ikawa, K. Santo, S. Sakai, H. Sato, S. Yamada, K. Hamaya, Electrical detection of spin accumulation and relaxation in *p*-type germanium, *Phys. Rev. Mater.* 1 (2017) 034604.
- [25] M. Yamada, F. Kuroda, M. Tsukahara, S. Yamada, T. Fukushima, K. Sawano, T. Oguchi, K. Hamaya, Spin injection through energy-band symmetry matching with high spin polarization in atomically controlled ferromagnet/ferromagnet/semiconductor structures, *NPG Asia Mater.* 12 (2020) 47.
- [26] K. Kudo, M. Yamada, S. Honda, Y. Wagatsuma, S. Yamada, K. Sawano, K. Hamaya, Room-temperature two-terminal magnetoresistance ratio reaching 0.1 % in semiconductor-based lateral devices with L_2 -ordered Co_2MnSi , *Appl. Phys. Lett.* 118 (2021) 162404.
- [27] A. Yamada, M. Yamada, M. Honda, S. Yamada, K. Sawano, K. Hamaya, Magnetoresistance ratio of more than 1 % at room temperature in germanium vertical spin-valve devices with Co_2FeSi , *Appl. Phys. Lett.* 119 (2021) 192404.
- [28] A. Toriumi, T. Nishimura, Germanium CMOS potential from material and process perspectives: Be more positive about germanium, *Japan. J. Appl. Phys.* 57 (2018) 010101.
- [29] H. Wu, P.D. Ye, Fully Depleted Ge CMOS Devices and Logic Circuits on Si, *IEEE Trans. Electron Device* 63 (2016) 3028–3035.
- [30] D. Wang, T. Maekura, S. Kamezawa, K. Yamamoto, H. Nakashima, Direct band gap electroluminescence from bulk germanium at room temperature using an asymmetric fin type metal/germanium/metal structure, *Appl. Phys. Lett.* 106 (2015) 071102.
- [31] R. Koerner, M. Oehme, M. Gollhofer, M. Schmid, K. Kostecki, S. Bechler, D. Widmann, E. Kasper, J. Schulze, Electrically pumped lasing from Ge Fabry-Perot resonators on Si, *Opt. Express* 23 (2015) 14815–14822.
- [32] K. Sawano, Y. Hoshi, S. Kubo, K. Arimoto, J. Yamanaka, K. Nakagawa, K. Hamaya, M. Miyao, Y. Shiraki, Structural and electrical properties of Ge(111) films grown on Si(111) substrates and application to Ge(111)-on-Insulator, *Thin Solid Films* 613 (2016) 24–28.
- [33] G. Schmidt, D. Ferrand, L.W. Molenkamp, A.T. Filip, B.J. van Wees, Fundamental obstacle for electrical spin injection from a ferromagnetic metal into a diffusive semiconductor, *Phys. Rev. B* 62 (R) (2000) R4790.
- [34] S. Takahashi, S. Maekawa, Spin injection and detection in magnetic nanostructures, *Phys. Rev. B* 67 (2003) 052409.
- [35] N. Matsuo, N. Doko, T. Takada, H. Saito, S. Yuasa, High Magnetoresistance in Fully Epitaxial Magnetic Tunnel Junctions with a Semiconducting GaO_x Tunnel Barrier, *Phys. Rev. Appl.* 6 (2016) 034011.
- [36] S. Kasai, Y.K. Takahashi, P.-H. Cheng, Ikhtiar, T. Ohkubo, K. Kondou, Y. Otani, S. Mitani, K. Hono, Large magnetoresistance in Heusler-alloy-based epitaxial magnetic junctions with semiconducting $\text{Cu}(\text{In}_{0.8}\text{Ga}_{0.2})\text{Se}_2$ spacer, *Appl. Phys. Lett.* 109 (2016) 032409.
- [37] S. Yamada, K. Tanikawa, M. Miyao, K. Hamaya, Atomically controlled epitaxial growth of single-crystalline germanium films on a metallic silicide, *Cryst. Growth Des.* 12 (2012) 4703–4707.
- [38] S. Sakai, M. Kawano, M. Ikawa, H. Sato, S. Yamada, K. Hamaya, Low-temperature growth of fully epitaxial CoFe/Ge/ Fe_3Si layers on Si for vertical-type semiconductor spintronic devices, *Semicond. Sci. Technol.* 32 (2017) 094005.
- [39] S. Gaucher, B. Jenichen, J. Kalt, U. Jahn, A. Trampert, J. Herfort, Growth of $\text{Fe}_3\text{Si}/\text{Ge}/\text{Fe}_3\text{Si}$ trilayers on $\text{GaAs}(001)$ using solid-phase epitaxy, *Appl. Phys. Lett.* 110 (2017) 102103.
- [40] M. Kawano, M. Ikawa, K. Arima, S. Yamada, T. Kanashima, K. Hamaya, All-epitaxial $\text{Co}_2\text{FeSi}/\text{Ge}/\text{Co}_2\text{FeSi}$ trilayers fabricated by Sn-induced low-temperature epitaxy, *J. Appl. Phys.* 119 (2016) 045302.
- [41] T. Shiihara, S. Oki, S. Sakai, M. Ikawa, S. Yamada, K. Hamaya, Epitaxial growth of Sb-doped Ge layers on ferromagnetic Fe_3Si for vertical semiconductor spintronic devices, *Semicond. Sci. Technol.* 33 (2018) 104008.
- [42] M. Honda, T. Shiihara, M. Yamada, S. Yamada, K. Hamaya, Germanium pn junctions between ferromagnetic CoFe and Fe_3Si layers for spintronic applications, *Mat. Sci. Semicon. Proc.* 116 (2020) 105066.
- [43] T. Shiihara, M. Yamada, M. Honda, A. Yamada, S. Yamada, K. Hamaya, Spin transport in antimony-doped germanium detected using vertical spin-valve structures, *Appl. Phys. Express* 13 (2020) 023001.
- [44] A. Yamada, M. Yamada, T. Shiihara, M. Ikawa, S. Yamada, K. Hamaya, Experimental estimation of the spin diffusion length in undoped *p*-Ge on Fe_3Si using vertical spin-valve devices, *J. Appl. Phys.* 129 (2021) 013901.
- [45] A.S. Tarasov, I.A. Tarasov, I.A. Yakovlev, M.V. Rautskii, I.A. Bondarev, A.V. Lukyanenko, M.S. Platunov, M.N. Volochaev, D.D. Efimov, A.Y. Goikhman, B.A. Belyaev, F.A. Baron, L.V. Shanidze, M. Farle, S.N. Varnakov, S.G. Ovchinnikov, N.V. Volkov, Asymmetric Interfaces in Epitaxial Off-Stoichiometric $\text{Fe}_{3+x}\text{Si}_{1-x}/\text{Ge}/\text{Fe}_{3+x}\text{Si}_{1-x}$ Hybrid Structures: Effect on Magnetic and Electric Transport Properties, *Nanomaterials* 12 (2022) 131.
- [46] S. Kusumoto, M. Yamada, A. Yamada, Y. Wagatsuma, K. Sawano, K. Hamaya, Structural and magnetic properties of CoFe/Sn-doped Ge/ Co_2FeSi for vertical spin-valve devices on Si, in: 2023 IEEE International Magnetic Conference - Short Papers (INTERMAG Short Papers), 2023, pp. 1–2.
- [47] M. Yamada, S. Kusumoto, A. Yamada, K. Sawano, K. Hamaya, Effect of Sn doping on low-temperature growth of Ge epilayers on half-metallic Co_2FeSi , *Mater. Sci. Semicond. Process.* 171 (2024) 107987.
- [48] A. Yamada, M. Yamada, S. Kusumoto, J.A. do Nascimento, C. Murrill, S. Yamada, K. Sawano, V.K. Lazarov, K. Hamaya, Growth of all-epitaxial $\text{Co}_2\text{MnSi}/\text{Ge}/\text{Co}_2\text{MnSi}$ vertical spin-valve structures on Si, *Mat. Sci. Semicon. Proc.* 173 (2024) 108140.
- [49] K. Hamaya, N. Hashimoto, S. Oki, S. Yamada, M. Miyao, T. Kimura, Estimation of the spin polarization for Heusler-compound thin films by means of nonlocal spin-valve measurements: Comparison of Co_2FeSi and Fe_3Si , *Phys. Rev. B* 85 (R) (2012) 100404.
- [50] T.M. Nakatani, T. Furubayashi, S. Kasai, H. Sukegawa, Y.K. Takahashi, S. Mitani, K. Hono, Bulk and interfacial scatterings in current-perpendicular-to-plane giant magnetoresistance with $\text{Co}_2\text{Fe}(\text{Al}_{0.5}\text{Si}_{0.5})$ Heusler alloy layers and Ag spacer, *Appl. Phys. Lett.* 96 (2010) 212501.
- [51] B. Büker, J. Jung, T. Sasaki, Y. Sakuraba, Y. Miura, T. Nakatani, A. Hüttner, K. Hono, Elucidation of the strong effect of an interfacial monolayer on magnetoresistance in giant magnetoresistive devices with current perpendicular to the plane, *Phys. Rev. B* 103 (2021) L140405.
- [52] Y. Fujita, Y. Miura, T. Sasaki, T. Nakatani, K. Hono, Y. Sakuraba, Spin-scattering asymmetry at half-metallic ferromagnet/ferromagnet interface, *Phys. Rev. B* 104 (2021) L140403.
- [53] T. Scheike, H. Sukegawa, K. Inomata, T. Ohkubo, K. Hono, S. Mitani, Chemical ordering and large tunnel magnetoresistance in $\text{Co}_2\text{FeAl}/\text{MgAl}_2\text{O}_4/\text{Co}_2\text{FeAl}(001)$ junctions, *Appl. Phys. Express* 9 (2016) 053004.
- [54] B. Hu, K. Moges, Y. Honda, H.X. Liu, T. Uemura, M. Yamamoto, J. Inoue, M. Shirai, Temperature dependence of spin-dependent tunneling conductance of magnetic tunnel junctions with half-metallic Co_2MnSi electrodes, *Phys. Rev. B* 94 (2016) 094428.
- [55] N. Tezuka, N. Ikeda, F. Mitsuhashi, S. Sugimoto, Improved tunnel magnetoresistance of magnetic tunnel junctions with Heusler $\text{Co}_2\text{FeAl}_{0.5}\text{Si}_{0.5}$ electrodes fabricated by molecular beam epitaxy, *Appl. Phys. Lett.* 94 (2009) 162504.
- [56] M. Ikawa, M. Kawano, S. Sakai, S. Yamada, T. Kanashima, K. Hamaya, Influence of the Ge diffusion on the magnetic and structural properties in Fe_3Si and CoFe epilayers grown on Ge, *J. Cryst. Growth* 468 (2017) 676–679.
- [57] K. Hamaya, T. Murakami, S. Yamada, K. Mibu, M. Miyao, Local structural ordering in low-temperature-grown epitaxial $\text{Fe}_{3+x}\text{Si}_{1-x}$ films on Ge(111), *Phys. Rev. B* 83 (2011) 144411.
- [58] S. Yamada, K. Yamamoto, K. Ueda, Y. Ando, K. Hamaya, T. Sadoh, M. Miyao, Epitaxial growth of a full-Heusler alloy Co_2FeSi on silicon by low-temperature molecular beam epitaxy, *Thin Solid Films* 518 (2010) S278–S280.